



# ANALYSIS ON CHARACTERISTICS AND INFLUENCING FACTORS OF VALLEY DEFORMATION OF HIGH ARCH DAM

**CHENG HENG, ZHANG GUOXIN, LIU YI, ZHOU QIUJING AND JIANG CHENFANG**

*China Institute of Water Resources and Hydropower Research, Beijing*

**ZHANG GUOXIN AND LIU YI**

*State Key Laboratory of Simulation and Regulation of Water Cycles in River Basin, Beijing*

**LIAO JIANXIN**

*China Three Gorges Corporation, Beijing*

## ABSTRACT

*At present, Valley shrinkage occurs in some high arch dams in China during impoundment, which may affect the working behavior and long-term safety of dams. In this paper, based on the monitoring data of the valley deformation of a high arch dam in China, the spatial-temporal distribution law of the deformation is analyzed. By establishing the multiple regression model of valley deformation, the process of valley deformation of each measuring line is analyzed by regression, and the influence factors of valley deformation are separated. On this basis, Combined with the specific engineering geological and hydrological geological conditions of dam site area, the influence factors of the valley deformation are analyzed. The result shows that the water pressure component, the water level's hysteresis effect component, and the temperature component in the measured valley deformation are small, most of which is time-dependent component. Under the specific hydrogeological conditions, the changing and adjustment of rock mass stress is the main inducing factors to valley shrinkage deformation in the process of seepage field's evolution.*

**Keywords:** *high arch dam; valley deformation; spatial-temporal distribution; aging deformation; influence factors*

## 1. INTRODUCTION

A high dam typically involves a high water head, high and steep bank slopes, and complex geological conditions. The original equilibrium state of the slopes is disrupted by excavation or water storage, inducing deformation in the slopes. Slope deformation has an important impact on the overall safety of hydropower works, a concern that has drawn wide attention among the dam community. There are a large number of bank slope deformation cases, both in China and abroad. The Beauregard arch dam (Italy), for instance, experienced gravity sliding deformation in the left bank slope in the early stage of water storage, with the sliding rate in proportion to the rise of the reservoir water level<sup>[1, 2]</sup>. Zeuzier Arch Dam, in Switzerland, after 21 years of normal operation, was diagnosed with seeping saturated rock mass, caused by the excavation of the Gotthard tunnel 400m beneath the dam base, which changed the base rock mass from a saturated into an unsaturated state, resulting in uneven settlement of the foundation and valley contraction<sup>[3-5]</sup>. The Maoping landslide body of the Geheyan Reservoir, on the Qingjiang River, began to deform after 1993, when the reservoir started to store water. By 2004, the cumulative horizontal displacement amounted to 2747.1mm and the vertical displacement to 548.4mm<sup>[6, 7]</sup>. The Laxiwa Hydropower Station, in China, developed toppling deformation on its bank following water storage. At present, the reservoir water has stabilized to the normal level. The maximum displacement of the front edge of the bank slope is about 40m, but the deformation is still growing, not fully checked<sup>[8]</sup>.

China's high-dam reservoirs have one after another entered their storage and operation stage. Some high arch dams, such as Jinping I, Xiluodu, and Lijiaxia, have developed valley shrinkage after storage--deformation towards the center of the valley. By April 2019, Xiluodu, in particular, has a maximum valley contraction, since storage, of about 93.47mm,

and the figure was 34.4mm in the case of the Liji Xia arch dam<sup>[9]</sup>. With the Jinping I, the maximum shrinkage was about 36 mm by March 2018. This figure is about 6.59mm in the case of Ertan<sup>[9]</sup>.

In view of the contraction cases of high arch dam valleys, domestic and foreign scholars, after analyzing its factors and causes, have suggested some explanations. Yang Jie et al<sup>[8]</sup> attribute the Liji Xia arch dam valley deformation to the shrinkage, the increased seepage pressure, and the decreased rock mass strength of the fracture zones under higher water pressure after water storage. The latest development of the valley deformation of the Xiluodu arch dam and the Jinping I arch dam has drawn intense attention among the dam community. Yang Qiang et al<sup>[11-13]</sup> analyze the deformation of the Jinping I arch dam valley from the perspective of effective stress change, pointing out that the fissure water pressure in the initial stage of water storage altered the equilibrium state of the rock mass and caused plastic deformation in the reservoir rock mass, which is the main driving force for the valley width deformation during water storage. Zhang Guoxin et al<sup>[14,15]</sup> assert that the deformation of the Xiluodu arch dam valley is mostly time-dependent, caused by altered hydrogeological conditions in the near-dam zone, which deformation is dominated by creep deformation. Zhou Zhifang et al<sup>[16]</sup> believe that under certain geological and hydrogeological conditions of the reservoir area, changed water pressure in the Yangxin limestone aquifer after water storage is the main cause of the deformation of the Xiluodu reservoir basin and its valley width. He Zhu et al.<sup>[17]</sup> argue that the additional seepage pressure and creep deformation of interlayer and inter-layer disturbed zones following water storage are the main causes of the deformation of the Xiluodu arch dam valley. Liang Guohe et al.<sup>[18]</sup> analyze the width deformation of Xiluodu arch dam valley and find that the correlation between valley contraction and reservoir water level and temperature is small, suggesting that there might be other factors. On the whole, existent studies focus mostly on qualitative analysis of the deformation mechanism, which is unable to give a full explanation for the characteristics and law of the deformation observed in the works.

These arch dam works have their own topography, stratum lithology, geological structure and hydrogeology. The law of their post-storage valley deformation varies from one another; so are the inducing factors of the deformation. The research on the origin and development of valley contraction is insufficient. Therefore, to reveal the temporal and spatial evolution law and the intrinsic dynamic mechanism of valley deformation it is necessary to review and analyze the deformation law and influencing factors of valley deformation of arch dams in different parts of the world. In this paper, typical cases in the world of high arch dam valley width deformation are reviewed, some valley deformation monitoring data are gathered and consolidated to develop and analyze the tempo-spatial distribution characteristics of the deformation in each case. Then, the monitoring data of the Xiluodu arch dam valley width are analyzed, to reveal the tempo-spatial evolution law of the deformation. The mechanism of the deformation of the valley is also discussed.

## 2. REVIEW OF TYPICAL HIGH ARCH DAM VALLEY WIDTH DEFORMATION CASES

### 2.1 Beaugard Arch Dam, Italy

Beaugard, a concrete gravity arch dam and 132m high, is located in the Aosta valley, northwestern Italy. In the left-bank slope there is a deep shear zone, composed of fragmented gneiss and fault mud. During the first years of water storage (1958--1968), gravity-sliding deformation occurred in the left bank slope, and over the 60 years after water storage the valley has shrunk 100mm to 200mm. Due to the large deformation in the left-bank slope, the sliding of the left-bank foundation caused the arch dam to be squeezed, making the dam to deform upstream (see Fig. 1) and inducing horizontal cracks on the downstream bottom (red lines in Fig. 2). The upstream horizontal joints then opened.

Having analyzing the long-term monitoring data, Barla<sup>[2]</sup> concludes that after the water level rose the shear strength of the deep shear zone fell, inducing the deformation. The fall of the shear strength of the deep shear zone, which happened after coming into contact with water, does not happen all at once. It is time-dependent.

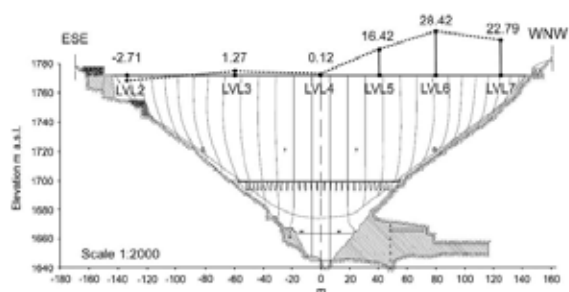


Fig. 1 : Deformation at the dam crest



Fig. 2 : Cracking of the downstream face of Beaugard Arch Dam

### 2.2 Zeuzier Arch Dam, Switzerland

Zeuzier Arch Dam is located in Sion, southwestern Switzerland. It is a concrete hyperbolic thin arch dam with a height of 156m. Its construction was completed in 1957 and the reservoir stored water in the same year. In 1976, a highway tunnel was built 400m beneath the dam base. Subsequent observation revealed noticeable foundation settlement and valley contraction, the latter reaching 60 mm. The contraction squeezed the dam causing its crest to deform upward by 110 mm. A number of cracks resulted, as shown in Fig. 4.

The settlement and valley deformation seen in the Zeuzier Arch Dam case are believed to be connected to the construction of the highway tunnel. When the work started on excavation of the tunnel, the seepage exceeded 1000L/s, a high seepage that drained the saturated rock mass and caused it to transit into an unsaturated state, ultimately leading to the dam foundation settlement and the valley contraction<sup>[3-5]</sup>.

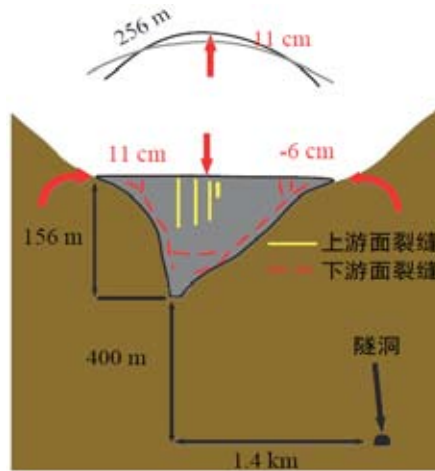


Fig. 4 : Schematic diagram of the overall deformation of the Zeuzier Arch Dam

### 2.3 Jinping Stage I Arch Dam

Jinping I Arch Dam sits on the main stream of the Yalong River, in Sichuan Province. The dam stands 305m high, with a crest elevation of 1885m. The normal water storage level is 1880m. From the lithological perspective, the dam site is made mainly of marble and sand slate. The foundation is characterized by ‘up-soft and down-hard’ on the left bank and ‘up-hard and down-soft’ on the right bank. Fig. 7 and 8 show the valley width deformation process line of the typical monitoring lines at some upstream, abutment and downstream points. The valley width monitoring lines were set up as shown in Fig. 5 and 6. It can be seen that at the initial stage of water storage there exists a good correlation between the upstream valley width deformation and the water level. A rising water level corresponds to apparent deformation. When the water level falls or stabilizes, the deformation slows down; the downstream valley width deformation is less affected by the water storage process and the deformation value is smaller than the upstream valley; In October 2016, when the water level reached the normal water level for the third time, the deformation rate observed along each monitoring line dropped evidently, with the deformation tending to converge. By March 2018, the upstream valley contraction reached a maximum of about 36mm, while the maximum downstream contraction was about 18mm.

Yang Qiang et al<sup>[11-13]</sup> analyze the valley width deformation mechanism of Jinping I Arch Dam from the perspective of effective stress change, pointing out that the fissure water pressure in the initial stage of water storage altered the equilibrium state of the rock mass and caused plastic deformation in the reservoir rock mass, which is the main driving force of the valley width deformation during water storage.

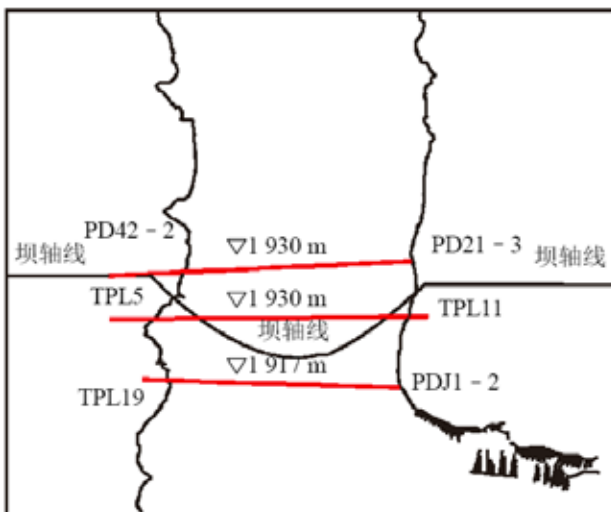


Fig. 5 : Upstream and abutment monitoring lines of valley width deformation

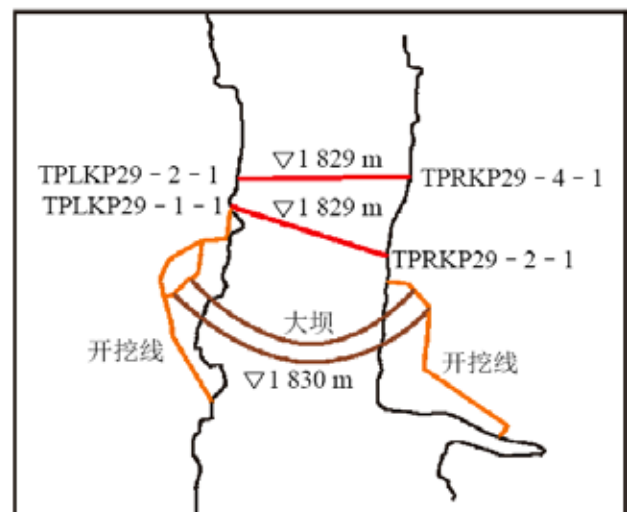


Fig. 6 : Downstream monitoring lines of valley width deformation

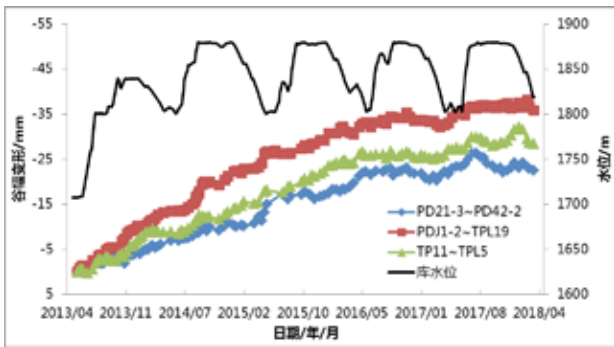


Fig. 7 : Deformation process lines of the upstream and abutment monitoring lines

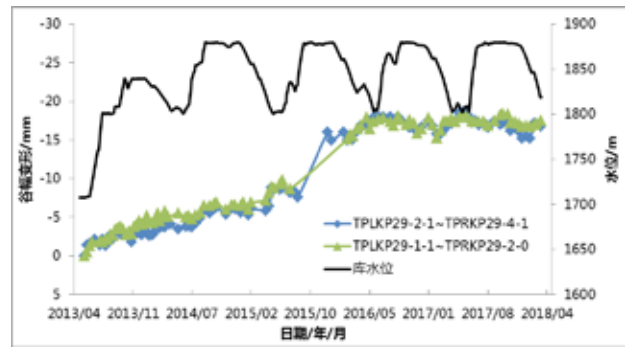


Fig. 8 : Deformation process lines of the downstream monitoring lines

## 2.4 Lijiaxia Arch Dam

This is a three-center double-curved arch dam, with a dam crest elevation of 2185m and a maximum height of 155m. The geological conditions of its reservoir and the dam site are complex, with developed geological structure and a number of weak foundation locations. There are some slope stability problems with the Lijiaxia reservoir area and the near-dam banks. The most prominent is the deformation in the left abutment and the downstream high slopes. There are established five valley width monitoring lines downstream of the arch dam, at an elevation of 2130~2185m, as shown in Table 1.

Table 1 : Arrangement of valley width monitoring points

Description	No. of monitoring points	Elevation (m)
Valley width monitoring	TP17~LJ03	2185
	LJ05~LJ07	2155
	TP15~LJ07	2160
	TP16~TP06	2155
	TP13~TP02	2130

Water storage began in December 1996 and continued until the beginning of 2002. The deformation process lines, developed from the five valley width monitoring lines, are given in Fig. 9. It can be seen that the five lines basically suggest the same deformation law--the valley contraction increases as the water level rises and, when the water level basically stabilizes at the normal water level, the deformation shows signs of convergence and stability. From the perspective of spatial distribution, the higher the elevation of the monitoring line, the greater the value of the observed deformation.

Yang Jie et al<sup>[10]</sup> analyze the displacement and safety status of the left-bank rock mass of Lijiaxia Arch Dam. It is suggested that there are obvious geological defects in the left reservoir bank near the dam. The increased seepage pressure and the decreased shear strength following water storage induced the gravity creep deformation of the bank slopes toward the center of the valley, causing the valley to contract.

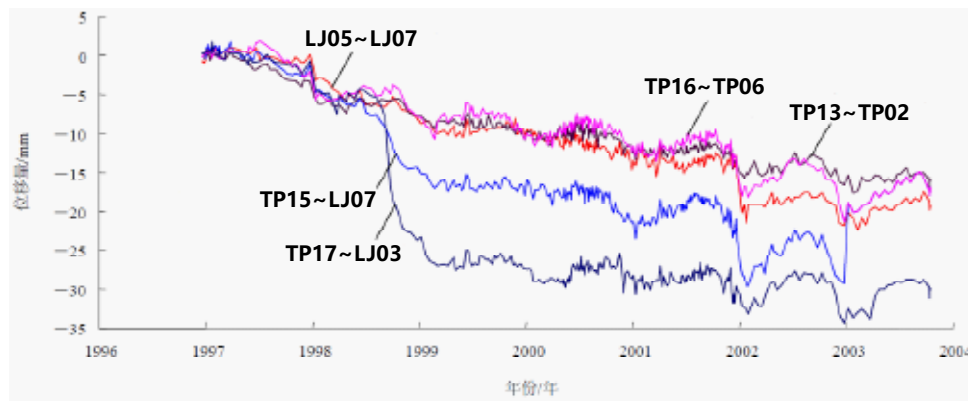


Fig. 9 : Process lines of measured valley deformation

The above analysis shows that, with a high water head, high and steep slopes, and complex geological conditions associated with a high dam, excavation or water storage alters the seepage field in the dam site, changing the hydrogeological



conditions. In the course of seepage field evolution, the change of effective stress on the rock mass structural planes and the softening of the rock mass after soaking are the main inducing factors of the contraction. The tempo-spatial distribution and evolution of the bank slope deformation are to a large extent affected by the geomorphology, stratum lithology, geological structure, and hydrogeology at the dam site. With the Xiluodu arch dam, obvious contraction deformation of the valley has been observed after water storage and, compared with those already observed in other arch dam cases, the deformation is greater, more extensive, and more complex in mechanism. Next, based on the monitoring data of the contraction deformation of the Xiluodu Arch Dam valley, we will analyze the tempo-spatial distribution of the deformation and, by factoring into the post-storage evolution of hydrogeological conditions of the dam site, explore the causes of the deformation.

### 3. ANALYSIS OF THE TEMPO-SPATIAL LAW OF THE WIDTH DEFORMATION OF THE XILUODU ARCH DAM VALLEY

Four upstream valley width monitoring lines (Line 01~04) and three downstream monitoring lines (Line 05~07) were set up, and an additional Line 08 in July 2014 and Line 09 in January 2016 were set up. The detailed layout of the monitoring lines is illustrated in Fig. 10. By April 2019, the upstream valley has narrowed by 69.42~93.47mm, the maximum value being observed at Line VDL03-VDR03, at an elevation of 722m. The downstream valley has narrowed by 78.83~80.51mm, and the maximum narrowing was at an elevation of 610m, observed along Line VDL06-VDR06. As far as spatial distribution goes, the contraction magnitudes of the upstream and downstream valleys are essentially the same, and the deformation varies very slightly along the elevation, with the deformation at a higher elevation being a little greater.

The elev. 559m monitoring line extends to the ADR20 and ADL20 drainage tunnels. The monitoring lines inside the two bank tunnels are both about 140m long, as shown in Fig. 11. By June 8, 2018, the valley had contracted by 37.73mm as measured at the tunnel openings. The tunnel opening monitoring point on the left bank shortened by 0.05mm relative to the monitoring point inside this tunnel. In the case of the right-bank tunnel, the narrowing was 0.89mm. All of this indicates that the relative displacements in both bank horizontal drainage tunnels are relatively small, suggesting that the contraction of the valley is not a superficial deformation but one present in a larger extent.

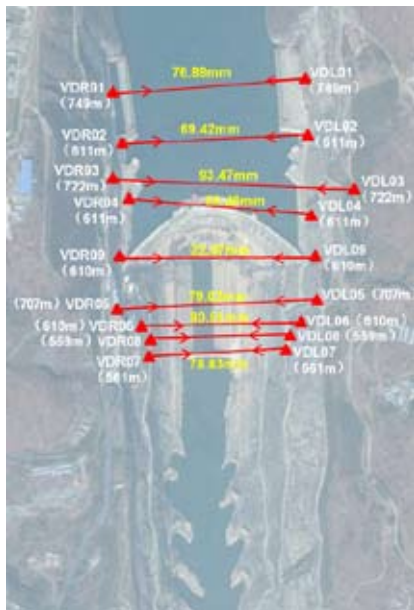


Fig. 10 : Schematic of the spatial distribution of the valley deformation

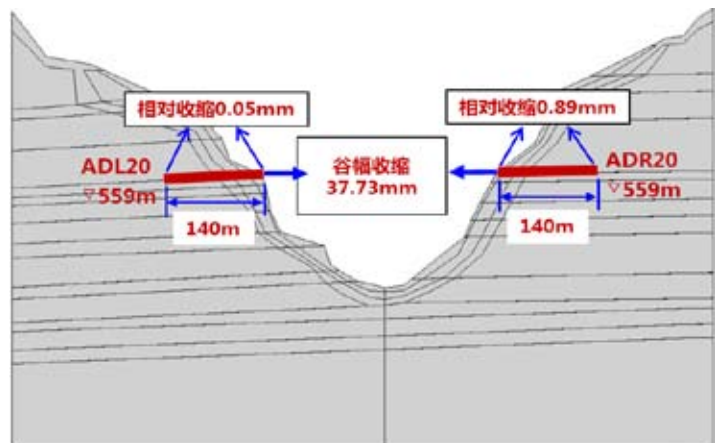


Fig. 11 : Valley width deformation observed in the ADL20-ADR20 drainage tunnels

Fig. 12 and 13 show the process lines of the deformations measured along the upstream and downstream monitoring lines. As can be seen, the valley contraction is not much connected with the water level, for the contraction does not decrease with the fall of the water level. The contraction continues after the reservoir is filled up with water. In May 2015, when the water level fell to its lowest level (545m) for the first time, the contraction trend slowed down clearly. At this moment, though the deformation has not converged, the rate is falling. A deformation process comparison between the upstream and downstream valleys suggests that contractions occurred synchronously upstream and downstream of the dam and were comparable in magnitude, implying that the effects of reservoir storage on the upstream and downstream bank slopes and dam foundation are synchronous.

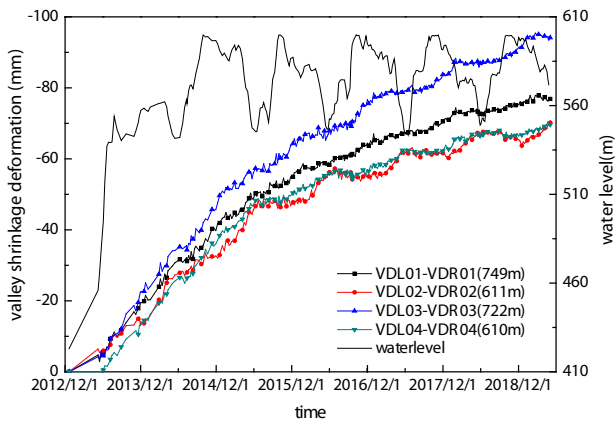


Fig. 12 : Process line of upstream valley contraction after water storage

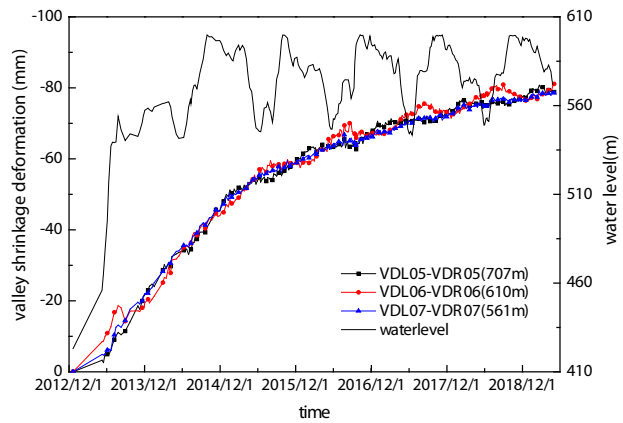


Fig. 13 : Process line of downstream valley contraction after water storage

## 4. ANALYSIS OF THE DEFORMATION CAUSES OF THE XILUODU ARCH DAM VALLEY

### 4.1 Hydrogeological conditions

Xiluodu Arch Dam is located in the Xiluodu gorge on Jinsha River, somewhere between Leibo County of Sichuan Province and Yongshan County of Yunnan Province. It is a concrete double-curvature arch dam with a height of 285.5m, a dam crest level of 610m and a normal water storage level of 600m. The dam bedrock and the slopes on both banks are mainly composed of basalt ( $P_2\beta$ ) and limestone ( $P_1m$ ), as shown in Fig. 14. The total thickness of the basalt is 490-520m. The limestone outcrops at the valley bottom bedrock, near the mouth of the Doushaxi river in the dam area, tilting downstream while plunging beneath the basalt. The limestone, as revealed by hole boring, is 260-280m thick. Between limestone and basalt is disposed a layer of shale deposits ( $P_2\beta n$ ), of 2~3m thick and with a maximum thickness of 5.1m. No large fractured fault is found near the dam site. Inter-layer and intra-layer fault zones are the prominent geological structures in the dam site area, which macroscopically dictate the layer-like structure and geotechnical behavior of the rock mass.

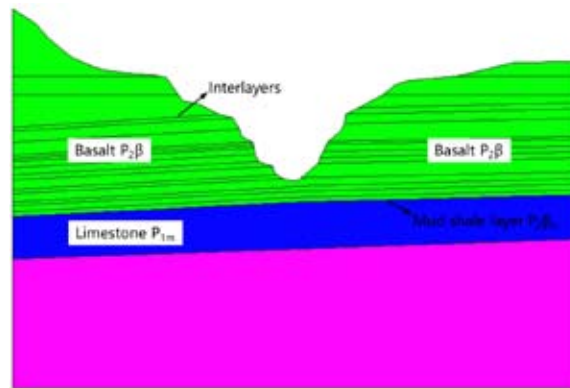


Fig. 14 : Hydrogeological cross section of Xiluodu dam site

Due to the deep-cut bottom fault around, the dam site area is in a regional geothermal anomaly zone. According to the riverbed borehole temperature data, the ground temperature increases with the depth. Generally, the influence of the river water is apparent within 10~20m below the bedrock surface and the temperature is low and varies appreciably, ranging between 18~25°C. As the depth grows, the temperature rises gradually, at a rate of about 3~5°C/100m owing to the geothermal warming effect. The limestone beneath the dam site contains groundwater with a higher temperature, which reaches 37~42°C at elevation 150~200m.

Fig. 15 shows a profile of the rock mass permeability at the Xiluodu dam site.  $P_2\beta$  basalt mostly has a weak to faint permeability ( $k < 3Lu$ ), with moderately permeable rock mass ( $k = 10 \sim 100Lu$ ) and weak to moderately permeable rock mass ( $k = 3 \sim 10Lu$ ) only appearing in unloaded zone and in interlayer and intra-layer disturbed zones. The  $P_1m$  limestone has more developed karst in the upstream outcrop area, while the limestone below the dam base is weakly developed in karst. In the riverbed, at the dam base, there is at the top of the limestone (205~250m in elevation and 30~50m in thickness) a downstream, sloping, tapering wedge-shaped rock mass (with a moderate permeability,  $k = 10 \sim 20Lu$ ), under which is a faintly permeable rock mass ( $k = 1 \sim 3Lu$ ). The  $P_2\beta n$  mud shale layer has a low permeability, thus a relatively water-tight formation.

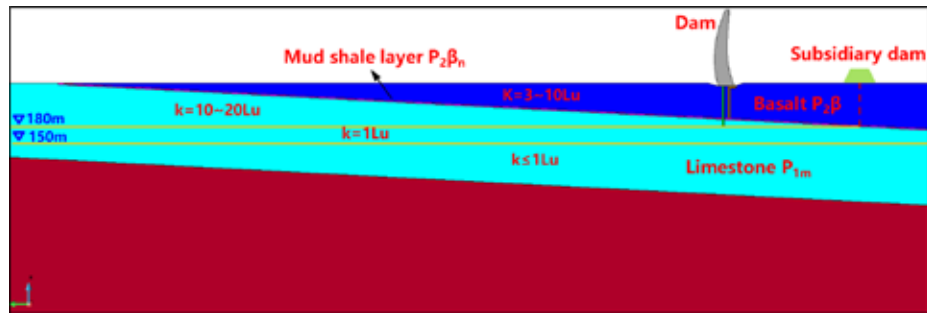


Fig. 15 : Zoning map of permeability profile of rock mass at Xiluodu dam site

## 4.2 Cause analysis

Following water storage, the seepage field in the dam site was altered, bringing about changes in the hydrogeological conditions. Factors inducing valley contraction may include:

(1) Changes in material properties. The groundwater level at the dam site was low before the commencement of construction, and bank slope rock mass was first in a dry or unsaturated state. Water infiltration following water storage drove up the water content of the rock mass, ultimately softening it. However, there are no large faults and weak rock belts in the Xiluodu dam site. Prominent structural planes are disturbed belts developed inside or between rock layers, and those disturbed belts are mostly filled with basalt breccia and fragments, with small inclusions of rock debris and virtually no mud. Moreover, generally the basalt in the dam site area is monolithic, with shallow weathering unloading, and thus has a high strength. The softening of the rock mass after water storage is of a weak degree, and therefore the softening of the rock mass is not the main cause of the valley contraction.

(2) Temperature change. The dam site being in a regional geothermal anomaly zone, the geothermal temperature of the underlying limestone is higher. Nevertheless, as the geothermal heat comes from deeper dam foundation, the reservoir water infiltration after storage merely cools down the superficial bedrock, without substantially altering the distribution of the geothermal field in the area. Therefore, the change in bedrock temperature is not the cause of the valley contraction.

(3) Stress changes. Some researchers measured the in-situ stress of the arch dam site before the dam construction<sup>[19, 20]</sup> (see Fig. 16 and Fig. 17). The geostress values suggest that the dam is at a medium geostress area, dominated by near-horizontal tectonic stress. The geostress field is of a generally balanced distribution, with the stress increasing with the depth. The measured maximum horizontal principal stress range between 11 and 16MPa (with a maximum of 20MPa), essentially parallel to the river stream. The measured minimum horizontal principal stress is 7-11 MPa, basically perpendicular to the stream. From about 40m below the riverbed center to  $P_2\beta_n$ , the stress increases rapidly, and stress concentration occurs at about an elevation of 270m. The minimum horizontal principal stress is 8MPa, while the maximum is 14MPa. Cake cores are developed in the limestone formation below  $P_2\beta_n$ , indicating a higher geostress, a larger difference between the major and minor principal stresses, and a greater shear stress.

Therefore, before water storage, the shear stress was great near the aquiclude  $P_2\beta_n$  below the dam base, probably in a critical equilibrium state, predisposing the rock mass to deform along the  $P_2\beta_n$  under extrusion. After water storage, with the seepage force acting on  $P_2\beta_n$ , the effective stress fell and the rock mass underwent disturbed deformation along  $P_2\beta_n$ , causing the valley to contract.

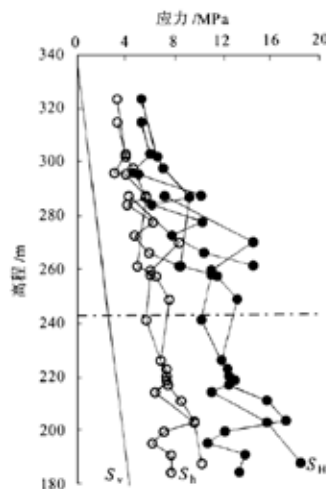


Fig. 16 : Horizontal principal stress vs. depth in 3 river center boreholes<sup>[19]</sup>

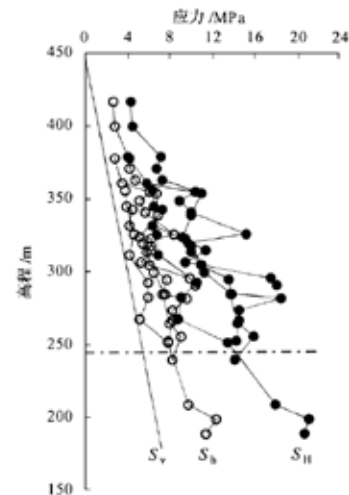


Fig. 17 : Horizontal principal stress vs. depth in 4 left-bank boreholes<sup>[19]</sup>

## 5. CONCLUSIONS

This paper reviews typical cases of high arch dam valley width contraction in the world and analyzes the tempo-spatial distribution characteristics and causes of such deformation, to find that the main inducing factors of valley width contraction are the change of effective stress on the rock mass structural planes during the evolution of the dam site seepage field after excavation or water storage and the softening of the rock mass. From this it continues to examine the valley width monitoring data of Xiluodu Arch Dam, shedding light on the temporal evolution and spatial distribution characteristics of the deformation. The mechanism of the deformation causes is then studied in the context of the engineering geology and hydrogeological conditions of the dam site. It is found that the contraction of the Xiluodu arch dam valley is great, and the contraction magnitudes of the upstream and downstream valleys are essentially the same, the deformation varying very slightly along the elevation, with the deformation at a higher elevation being a little greater. The valley contraction is not much related to the water level, for the contraction continued after the reservoir was filled up with water. At this point, though the deformation has not converged, the rate is falling. Before water storage, the shear stress was great near the aquiclude P2βn below the dam base, probably in a critical equilibrium state, predisposing the rock mass to deform along the P2βn under extrusion. After water storage, with the seepage force acting on P2βn, the effective stress fell and the rock mass underwent disturbed deformation and creeping deformation along P2βn, ultimately causing the valley to shrink.

## Acknowledgement

This work was supported by the National Key Research and Development Project of China(2018YFC0406700); China Three Gorges Corporation Research Project (XLD/2114); National Natural Science Foundation of China (51779277).

## REFERENCES

- [1] Frigerio A, Mazza G. The rehabilitation of Beauregard dam: the contribution of the numerical modeling. 12th International Benchmark Workshop on Numerical Analysis of Dams, Graz, Austria. 2013, 343-352.
- [2] Barla G, Antolini F, Barla M, et al. Monitoring of the Beauregard landslide(Aosta Valley, Italy) using advanced and conventional techniques[J]. *Engineering Geology*, 2010, 116(3): 218-235.
- [3] Lombardi E G. Ground-water induced settlements in rock masses and consequences for dams[C]//IALAD-Integrity Assessment of Large Concrete Dams Conference, Zurich. 2004, 24.
- [4] Zangerl C, Evans K F, Eberhardt E, et al. Consolidation settlements above deep tunnels in fractured crystalline rock: Part 1—Investigations above the Gotthard highway tunnel[J]. *International Journal of Rock Mechanics and Mining Sciences*, 2008, 45(8): 1195-1210.
- [5] Ehrbar H, Bremen R, Otto B. Gotthard Base tunnel-Tunnelling in the influence zone of two concrete arch dams[J]. *Geomechanics and Tunnelling*, 2010, 3(5): 428-441.
- [6] Yan Fuzhang, Wang Sijing, Xu Ruichun. Deformation mechanism and development tendency of Maoping Landslide after impounding of Geheyan reservoir on Qingjiang river[J]. *Journal of Engineering Geology*, 2003(01): 15-24.
- [7] Li Shouding, Li Xiao, Liu Yanhui. Study on generation and evolution of Maoping landslide on Qingjiang river [J]. *Chinese journal of rock mechanics and engineering*, 2006, 25(2): 377-384.
- [8] Zhang Haiping. Stability prediction and instability forecasting of the Guobo bank slope of the Laxiwa Hydropower Station on the Yellow River [D]. Chengdu: Chengdu University of Technology, 2011.
- [9] Wu Mingxin, Jiang Hui, Zhang Chuhan. General rules of dam-valley deformation due to reservoir impoundment [J]. *Journal of hydroelectric engineering*, 2019, 38(8): 1-14.
- [10] Yang Jie, Hu Dexiu, Guan Wenhui. Analysis of High Slope Rock Deformation and Safety Performance for Left Bank of Lijiaxia Arch Dam[J]. *Chinese Journal of Rock Mechanics and Engineering*, 2005, 24(19): 3551-3560.
- [11] Yang Qiang, Pan Yuanwei, Cheng Li, et al. Mechanism of Valley Deformation of High Arch Dam and Effective Stress Principle for Unsaturated Fractured Rock Mass[J].*Chinese Journal of Rock Mechanics and Engineering*, 2015,34(11):2258-2269.
- [12] Yang Qiang, Pan Yuanwei, Cheng Li, Liu Yaoru. Impounding influence of slope and foundation deformation on high arch dam[J]. *Chinese journal of rock mechanics and engineering*, 2015, 34(suppl.-2): 3979-3986.
- [13] L. Cheng, Y.R. Liu, Q. Yang, Y.W. Pan, Z. Lv. Mechanism and numerical simulation of reservoir slope deformation during impounding of high arch dams based on nonlinear FEM[J]. *Computers and Geotechnics*, 2017, 81: 143-154.
- [14] Zhang Guoxin, Cheng Heng, Zhou Qiuqing, Liu Youzhi. Analysis of mechanism of valley creep deformation of high arch dam during impoundment [J]. *China sciencepaper*, 2019, 14(1): 77-84.
- [15] LIU Youzhi, ZHANG Guoxin, CHENG Heng, et al. High arch dam of the narrow valley causes and the influence on dam deformation and stress analysis[C]. 2014 annual conference of Chinese national committee on large dams. Zhengzhou: The yellow river conservancy press, 2014:51-60.



- [16] Zhou Zhifang, Li Mingwei, Zhuang Chao, Guo Qiaona. Impact factors and forming conditions of valley deformation of Xiluodu hydropower station[J]. Journal of Hohai University, 2018, 46(6): 497-505.
- [17] He Zhu, Liu Yaoru, Yang Qiang, Cheng Li, Xue Lijun. Mechanism of valley deformation of Xiluodu arch dam and back analysis and long-term stability analysis[J]. Chinese Journal of Rock Mechanics and Engineering, 2018, 37(supple.-2): 4198-4206.
- [18] LIANG Guohe, HU Yu, FAN Qixiang, et al. Analysis on valley deformation of Xiluodu high arch dam during impoundment and its influencing factors[J].Journal of Hydroelectric Engineering, 2016, 35(9): 101-110.
- [19] Ding Lifeng, An Qimei, Wang Haizhong, Zhao Shiguang. Research on crustal stress measurement with hydrofracturing in the Xiluodu Hydropower Station on the Jinsha river[J]. Earthquake Research in China, 2004, 20(1): 95-100.
- [20] Ding Lifeng, An Qimei, Wang Haizhong, Zhao Shiguang, WANG Haizhong[J]. Hydrogeology and Engineering Geology, 2004, (6): 56-59.